Reduction of Finite Element Models of Complex Mechanical Components

Håkan Jakobsson
Research Assistant
hakan.jakobsson@math.umu.se

Mats G. Larson
Professor Applied Mathematics
mats.larson@math.umu.se

Gabriel Granåsen
Research Assistant

Department of Mathematics and Mathematical Statistics,
Umeå University, S-901 87 Umeå, Sweden

Abstract

There is an increasing interest in using detailed finite element models of individual components in multibody simulation with detailed contact analysis. Due to the large amount of degrees of freedoms in such models we need to develop reduced models with fewer degrees of freedoms that still capture the flexible body dynamics with sufficient accuracy. In this paper we investigate a static load case on a geometrically complex mechanical component. We use modal basis functions to describe the global deformations of the component and certain Krylov-modes to capture a localized load and to provide accurate coupling to the modal basis functions. We investigate how the overall accuracy depends on the number of modal basis functions and the number of Krylov-modes.

1. Introduction

Dynamics simulation involving complex finite element models is computationally demanding despite the rapid development of computational resources. To reduce computational cost, model reduction techniques are commonly employed. There are several classical model reduction techniques. See for instance [1] for a detailed description on the use of model reduction in structural dynamics. See also [2] for an account of model reduction in context of multibody dynamics.

Commonly reduction techniques are based on the assumption that a deformable object in a simulation is affected by boundary loads at a fixed number of specified points only, where the object is connected to its surroundings through so called coupling elements, e.g., springs, dampers and joints. In the general multibody setting this may however not be the case. Here objects may in addition be affected by contact forces originating from dynamic collisions with other objects. These collisions may occur at arbitrary points, and the contact forces may be moving, e.g., a rolling bearing simulation.

This paper is the first in a series documenting a research effort towards finding new model reduction techniques that may be applied in the general multibody setting with geometrically complex deformable objects. The initial aim is to identify suitable correction modes that can be computed on the fly, or in a post processing step, in order to improve the convergence of a modal based reduction in a continuous manner. To this end we investigate in this paper static deformation of a geometrically complex elastic body with a localized boundary load. We use eigenmodes to capture low frequency global effects, and compute certain Krylov-modes to capture high frequency effects stemming from the boundary load. The Krylov-modes we generate are L_2-orthogonal to the eigenmodes per construction, thus removing the computational overhead associated with orthogonalization against these. We illustrate the effect of the Krylov-modes in a numerical study. N.b. Krylov-modes are commonly used in Krylov subspace methods for the iterative solution of large, sparse, linear systems of equations. Typically such methods seek approximate solutions to $m \times m$ linear system of equations $\boldsymbol{A}\boldsymbol{x} = \boldsymbol{b}$ in subspaces $\mathcal{K}_k(\boldsymbol{A}, \boldsymbol{b}) = \text{span}\,\{\boldsymbol{A}^{i-1}\boldsymbol{b}\}_{i=1}^{k}$, of $\mathbf{R}^m$ cf. [3]. These are natural subspaces to seek approximate solutions in. In fact, if $\boldsymbol{A}$ is invertible it follows that $\boldsymbol{x} = \boldsymbol{A}^{-1}\boldsymbol{b} \in \mathcal{K}_n(\boldsymbol{A}, \boldsymbol{b})$, where n is the degree of the minimal polynomial of $\boldsymbol{A}$.

The paper is organized as follows. In Section 2 we outline the theory associated with modal based model reduction techniques and define the specific Krylov-modes we use in our computations. In Section 3 we perform a numerical study and discuss some aspects of mesh refinement. In Section 4 we summarize the results and outline the continuation of these works.

2. Theoretical Investigation

2.1 The Equations of Linear Elasticity

We consider the equations of linear elasticity in two dimensions: find the vector displacement $\boldsymbol{u} = [u_i]_{i=1}^2$ and

the symmetric stress tensor $\boldsymbol{\sigma} = [\sigma_{ij}]_{i,j=1}^2$ such that

$$\begin{aligned} -\nabla \cdot \boldsymbol{\sigma}(\boldsymbol{u}) &= \mathbf{0}, \quad x \in \Omega, \\ \boldsymbol{\sigma} &= 2\mu\boldsymbol{\varepsilon}(\boldsymbol{u}) + \lambda(\nabla \cdot \boldsymbol{u})\boldsymbol{I} \quad x \in \Omega, \\ \boldsymbol{u} &= \mathbf{0}, \quad s \in \Gamma_D, \\ \boldsymbol{n} \cdot \boldsymbol{\sigma} &= \boldsymbol{h}, \quad s \in \Gamma_N, \end{aligned} \tag{1}$$

where Ω is a closed subset of $\mathbf{R}^2$, Γ_D and Γ_N are parts of the boundary, $\partial\Omega$, such that $\Gamma_D \cup \Gamma_N = \partial\Omega$ and $\Gamma_D \cap \Gamma_N = \emptyset$. Furthermore, $\boldsymbol{\varepsilon}(\boldsymbol{u}) = [\varepsilon_{ij}]_{i,j=1}^2$ is the strain tensor with components

$$\varepsilon_{ij}(u) = \frac{1}{2}\left(\frac{\partial u_i}{\partial x_j} + \frac{\partial u_j}{\partial x_i}\right), \tag{2}$$

$\nabla \cdot \boldsymbol{\sigma} = \left[\sum_{j=1}^2 \partial\sigma_{ij}/\partial x_j\right]_{i=1}^2$, $\boldsymbol{I} = [\delta_{ij}]_{i,j=1}^2$ with δ_{ij} the Kronecker delta, $\boldsymbol{h}$ is a given traction load, and $\boldsymbol{n}$ is an outward pointing unit normal. Lastly, λ and μ are the Lamé parameters satisfying $0 < \mu_1 < \mu < \mu_2$ and $0 < \lambda < \infty$. In the case of plane strain we have $\lambda = E\nu/((1+\nu)(1-2\nu))$ and $\mu = E/(2(1+\nu))$, where E is Young's elastic modulus and ν Poisson's ratio.

2.2 The Finite Element Method

The weak formulation of (1) reads: Find $\boldsymbol{u} \in \mathcal{V}_{\mathbf{0}} = \{\boldsymbol{v} \in H^1[\Omega]^2 : \boldsymbol{v}|_{\Gamma_D} = \mathbf{0}\}$ such that

$$a(\boldsymbol{u}, \boldsymbol{v}) = b(\boldsymbol{v}), \quad \forall \boldsymbol{v} \in \mathcal{V}_{\mathbf{0}}, \tag{3}$$

where the linear forms $a(\cdot,\cdot)$, and $b(\cdot)$ are defined by

$$\begin{aligned} a(\boldsymbol{v}, \boldsymbol{w}) = 2(\mu\boldsymbol{\varepsilon}(\boldsymbol{v}) : \boldsymbol{\varepsilon}(\boldsymbol{w})) \\ + (\lambda\nabla \cdot \boldsymbol{v}, \nabla \cdot \boldsymbol{w}), \end{aligned} \tag{4}$$

$$b(\boldsymbol{v}) = (\boldsymbol{h}, \boldsymbol{v}). \tag{5}$$

In order to set up the finite element method, let $\mathcal{T}^h = \{T\}$ be subdivision of Ω into triangular elements T, and let $\mathcal{V}_{h,\mathbf{0}} = \{\boldsymbol{v} \in H^1(\Omega)^2 : \boldsymbol{v}|_T \in \mathbf{P}(T)^k, \boldsymbol{v}|_{\Gamma_D} = \mathbf{0}\}$, with $k = 1$ or $k = 2$, be an N-dimensional subspace to $[H^1(\Omega)]^2$. In the finite element method we seek an approximate solution $\boldsymbol{u}_h \in \mathcal{V}_{h,\mathbf{0}}$ such that

$$a(\boldsymbol{u}_h, \boldsymbol{v}) = b(\boldsymbol{v}), \quad \forall \boldsymbol{v} \in \mathcal{V}_{h,\mathbf{0}}. \tag{6}$$

Given a basis $\{\boldsymbol{\varphi}_j\}_{j=1}^N$ to $\mathcal{V}_{h,\mathbf{0}}$, this problem is equivalent to an $N \times N$ linear system of equations

$$\boldsymbol{K}\hat{\boldsymbol{u}}_h = \hat{\boldsymbol{b}}, \tag{7}$$

with elements

$$K_{ij} = a(\boldsymbol{\varphi}_j, \boldsymbol{\varphi}_i), \quad i,j = 1,\ldots,N, \tag{8}$$

$$b_i = b(\boldsymbol{\varphi}_i), \quad i = 1,\ldots,N. \tag{9}$$

2.3 The Model Reduction

In 3D dynamics simulation with flexible bodies accurate approximation of deformation and stresses comes with a significant computational cost. The system of equations corresponding to (7) is likely to contain a very large number of degrees of freedoms and require extensive computational resources to solve. To reduce the computational cost model reduction techniques are commonly employed.

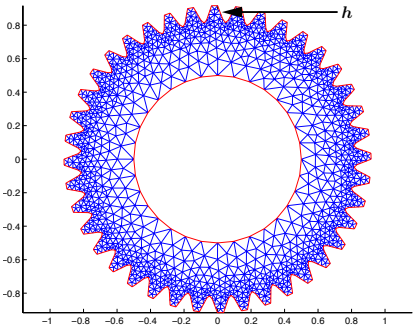

Figure 1: Localized force acting on domain boundary.

We investigate a static two-dimensional example. Consider therefore the situation illustrated in Figure 1, where a localized load acts on the boundary of a geometrically complex domain, a two-dimensional gear wheel with 40 teeth. Even in 2D, the system (7) will contain a significant number of degrees of freedoms and a model reduction is justified. This means that we must try to find a subspace $\mathcal{V}_{h,R} \subset \mathcal{V}_{h,\mathbf{0}}$ such that $n = \dim \mathcal{V}_{h,R} \ll \dim \mathcal{V}_{h,\mathbf{0}}$ and such that $\|\boldsymbol{u}_{h,R} - \boldsymbol{u}_h\|_{H^1(\Omega)^2}$ is small, where $\boldsymbol{u}_{h,R} \in \mathcal{V}_{h,R}$ satisfies

$$a(\boldsymbol{u}_{h,R}, \boldsymbol{v}) = b(\boldsymbol{v}), \quad \forall \boldsymbol{v} \in \mathcal{V}_{h,R}. \tag{10}$$

It is obvious that it is hard to construct a general such space $\mathcal{V}_{h,R}$. If we however exploit our knowledge of $\boldsymbol{h}$ we can tune $\mathcal{V}_{h,R}$ according to the specific load case.

Therefore, let $\mathcal{V}_{h,R} = \mathcal{V}_{h,TM} \oplus \mathcal{V}_{h,K}$, where $\mathcal{V}_{h,TM} \subset \mathcal{V}_{h,\mathbf{0}}$ is a space spanned by a subset of the eigenvectors of a, and $\mathcal{V}_{h,K} \subset \mathcal{V}_{h,\mathbf{0}}$ a Krylov-space. The space $\mathcal{V}_{h,TM}$ is chosen as to capture global deformations, and the space $\mathcal{V}_{h,K}$ is chosen to capture localized high-frequency effects in a neighborhood around the applied boundary load.

We first consider the space $\mathcal{V}_{h,TM}$. Since a is a symmetric bilinear form on $\mathcal{V}_{h,\mathbf{0}}$, the eigenmodes corresponding to the eigenvalue problem

$$a(\boldsymbol{e}_h, \boldsymbol{v}) = \lambda \int_\Omega \boldsymbol{e}_h \boldsymbol{v}\, d\boldsymbol{x}, \quad \forall \boldsymbol{v} \in \mathcal{V}_{h,0}, \tag{11}$$

form an orthogonal basis in $\mathcal{V}_{h,\mathbf{0}}$. Since we want to capture only the low-frequent, global behavior of the body

with eigenmodes, we let $\mathcal{V}_{h,TM}$ be the space spanned by the truncated modal basis (cf. [1]), $\{\boldsymbol{e}_h^i\}_{i=1}^m$, where $\boldsymbol{e}_h^i$, $i = 1, \ldots, m$ are the eigenmodes corresponding to the m smallest eigenvalues of a.

Now, the eigenvalue problem (11) is equivalent to a linear system of equations

$$\boldsymbol{K}\hat{\boldsymbol{e}}_h = \lambda \boldsymbol{M}\hat{\boldsymbol{e}}_h, \tag{12}$$

where $\boldsymbol{M}$ is the mass matrix. We find the low-frequency component, $\boldsymbol{u}_{h,TM}$, of our reduced solution by solving the $m \times m$ system of equations

$$\boldsymbol{V}_{h,TM}^T \boldsymbol{K} \boldsymbol{V}_{h,TM} \hat{\boldsymbol{u}}_{h,TM} = \boldsymbol{V}_{h,TM}^T \hat{\boldsymbol{b}}, \tag{13}$$

for its coefficients $\hat{\boldsymbol{u}}_{h,TM} = [u_{1,TM}, \ldots, u_{m,TM}]^T$, where $\boldsymbol{V}_{h,TM}$ is an $N \times m$ matrix with the m most low-frequent eigenmodes from (12) in its columns.

In order to capture the local effects we introduce the space $\mathcal{V}_{h,K}$, defined by the $N \times k$ coefficient matrix $\boldsymbol{V}_{h,K}$, with column vectors

$$\hat{\boldsymbol{c}}_j = \left[(\boldsymbol{M}^{-1}\boldsymbol{K})^j \boldsymbol{M}^{-1} \boldsymbol{r}_{TM}\right]_{j=0}^{k}, \tag{14}$$

where $\boldsymbol{r}_{TM}$ is the residual stemming from the eigenmode approximation. That is,

$$\boldsymbol{r}_{TM} = \hat{\boldsymbol{b}} - \boldsymbol{V}_{h,TM}\hat{\boldsymbol{u}}_{h,TM}, \tag{15}$$

where $\hat{\boldsymbol{u}}_{h,TM}$ is the solution to the system (13). The Krylov-modes thus generated are per construction orthogonal to the truncated modal basis. This approach can be compared with the so called modal acceleration method, cf. [1], where in fact the generating operator is the inverse to the operator in (14) above.

We find the high-frequency component, $\boldsymbol{u}_{h,K}$, of the reduced solution by solving the $k \times k$ system of equations

$$\boldsymbol{V}_{h,K}^T \boldsymbol{K} \boldsymbol{V}_{h,K} \hat{\boldsymbol{u}}_{h,K} = \boldsymbol{V}_{h,K}^T \hat{\boldsymbol{b}}, \tag{16}$$

for the coefficients $\hat{\boldsymbol{u}}_{h,K} = \{u_{1,K}, \ldots, u_{k,K}\}$, and our reduced solution is $\boldsymbol{u}_{h,R} = \boldsymbol{u}_{h,TM} + \boldsymbol{u}_{h,K}$.

3. Numerical Investigations

3.1 Numerical Results

To illustrate the ideas described above we present the following numerical investigation of how the accuracy in the computation depends on the number of eigenmodes and the number of Krylov-modes in the reduction basis. The computational domain is depicted in Figure 1. We apply the localized force as illustrated in the same figure. We use the elastic modulus $E = 1.0$, and Poisson's ratio $\nu = 0.29$.

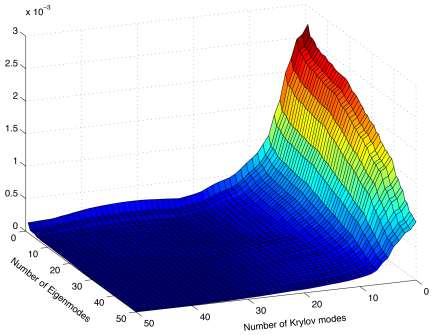

(a) The max-norm error $E_{i,j}^{L_\infty}(\boldsymbol{u}_h)$ on the deformation.

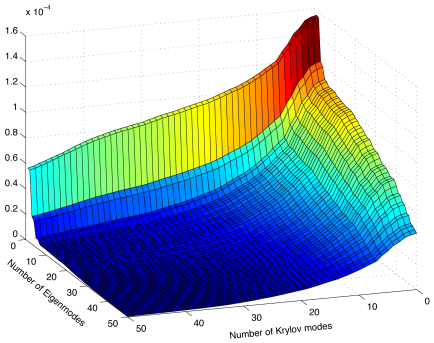

(b) The L_2 error $E_{i,j}^{L_2}(\boldsymbol{u}_h)$ on the deformation.

Figure 2: Errors on the deformation for $i = 1, \ldots, 50$ eigenmodes, and $j = 0, \ldots, 50$ Krylov-modes, respectively.

Let $\mathcal{V}_{h,R(i,j)}$ be the reduced space spanned by the first i eigenmodes and the first j Krylov-modes respectively, and let $\boldsymbol{u}_{h,R(i,j)}$ be the corresponding solution. We compute the maximum-norm errors

$$\begin{aligned} E_{i,j}^{L_\infty}(\boldsymbol{u}_h) =& \|\boldsymbol{u}_{h,R(i,j)} - \boldsymbol{u}_h\|_{L_\infty(\Omega)}, \\ & i = 1, \ldots, 50,\ j = 0, \ldots, 50, \end{aligned} \tag{17}$$

and the L_2-errors

$$\begin{aligned} E_{i,j}^{L_2}(\boldsymbol{u}_h) =& \|\boldsymbol{u}_{h,R(i,j)} - \boldsymbol{u}_h\|_{L_2(\Omega)}, \\ & i = 1, \ldots, 50,\ j = 0, \ldots, 50, \end{aligned} \tag{18}$$

between a reference FEM solution and a set of reduced solutions. The results from these computation are depicted in Figure 2. It is clear from the graphs that the truncated modal basis alone is not able to resolve the load case in a satisfactory way, and that the error is reduced effectively by the addition of Krylov-modes to the basis. It is also clear from graph (b) that it is necessary to keep some eigenmodes in the basis in order to capture global effects. Let $\sigma_{h,R(i,j)}^v$ and σ_h^v denote the von Mises stresses corresponding to the reduced solution and the

FEM solution respectively. The maximum-norm errors

$$E^{L_2}_{i,j}(\sigma^v_h) = \|\sigma^v_{h,R(i,j)} - \sigma^v_h\|_{L_\infty(\Omega)}, \quad i = 1,\dots,50,\ j = 0,\dots,50, \tag{19}$$

in the von Mises stresses, are plotted in Figure 3. It is clear from this figure that the Krylov-modes significantly enhances the von Mises approximation. In Figure 4, we see the von Mises stresses corresponding to the reference solution $\boldsymbol{u}_h$, a reduced solution $\boldsymbol{u}_{h,R(20,10)}$ and a reduced solution $\boldsymbol{u}_{h,R(30,0)}$ respectively.

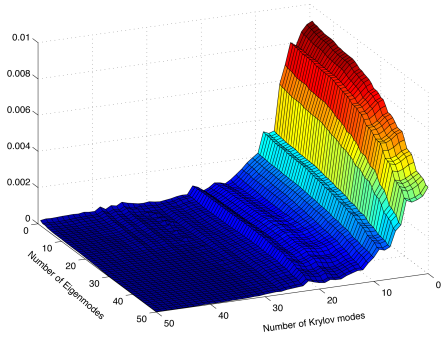

Figure 3: The maximum-norm error $E^{L_\infty}_{i,j}(\sigma^v_h)$ in the von Mises stresses, for $i = 1,\dots,50$ eigenmodes, and $j = 0,\dots,50$ Krylov-modes, respectively.

3.2 Aspects of mesh refinement

By subtracting (6) from (3) we get the Galerkin orthogonality:

$$a(\boldsymbol{u} - \boldsymbol{u}_h, \boldsymbol{v}) = 0, \quad \forall \boldsymbol{v} \in \mathcal{V}_h. \tag{20}$$

The analog Galerkin orthogonality for the reduced solution is attained by subtracting (10) from (6):

$$a(\boldsymbol{u}_h - \boldsymbol{u}_{h,R}, \boldsymbol{v}) = 0, \quad \forall \boldsymbol{v} \in \mathcal{V}_{h,R}. \tag{21}$$

From (20) and (21) now follows

$$\|\boldsymbol{u} - \boldsymbol{u}_{h,R}\|^2_E = \|\boldsymbol{u} - \boldsymbol{u}_h\|^2_E + \|\boldsymbol{u}_h - \boldsymbol{u}_{h,R}\|^2_E, \tag{22}$$

were $\|\cdot\|_E$ denotes the energy norm, defined by

$$\|\boldsymbol{w}\|^2_E = a(\boldsymbol{w}, \boldsymbol{w}), \quad \forall \boldsymbol{w} \in \mathcal{V}_0. \tag{23}$$

Looking at (22) it's apparent that given a fixed set of reduction modes, the left hand side will be approximately constant (compared to the variation in h). The second term on the right hand side will hence grow larger as h tends to zero. This means that a greater number of reduction modes is needed if the geometry is complex and the mesh has fine-scale features.

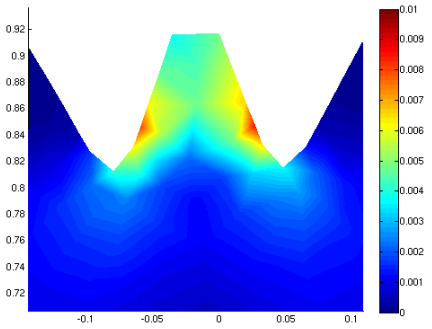

(a) Von Mises stresses on the reference solution $\boldsymbol{u}_h$.

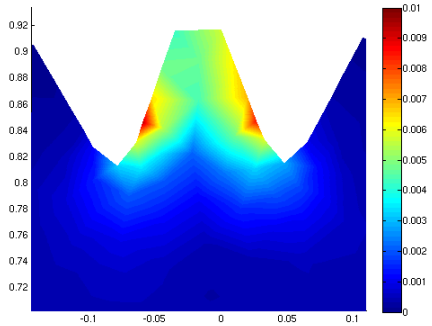

(b) Von Mises stresses on a reduced solution $\boldsymbol{u}_{h,R(20,10)}$, using 20 eigenmodes and 10 Krylov-modes.

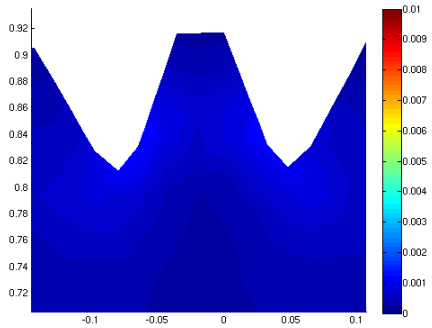

(c) Von Mises stresses on a reduced solution $\boldsymbol{u}_{h,R(30,0)}$, using 30 eigenmodes and 0 Krylov-modes.

Figure 4: Von Mises stresses on the reference and reduced solutions.

In order to see how this manifests itself in the numerical results we compute the von Mises stresses on a reference FE solution $\boldsymbol{u}_h$ and a reduced solution $\boldsymbol{u}_{h,R(20,10)}$ with 20 eigenmodes and 10 Krylov-modes on a mesh locally refined as in Figure 5.

The Mises stresses around the loaded tooth of the reference FEM solution and the reduced solution can be seen in Figure 6. Compare this with the corresponding result on the coarse mesh in Figure 4. On the refined mesh it is apparent that 20 eigenmodes and 10 Krylov-modes in the reduction space is not enough to capture FE solution. We see that the effect of the Krylov-modes

here is somewhat too local.

Now, the addition of more Krylov-modes to the basis will not improve the reduction significantly since the locality of the Krylov-modes will increase with k, and we know that the computation of more eigenmodes is expensive. Research is currently being undertaken in order to identify an effective approach to resolve this matter.

3.3 Notes on the Implementation

We have implemented the above computations in MATLAB [4] using the Standard Galerkin [5] method on a triangular mesh with linear basis functions. For fast Krylov-mode generation we have used a lumped mass matrix in the computations. The Krylov-modes are generated using the Arnoldi Modified Gram-Schmidt algorithm [3]. The eigenvalue problem is solved using ARPACK [6] through the MATLAB command `eigs`.

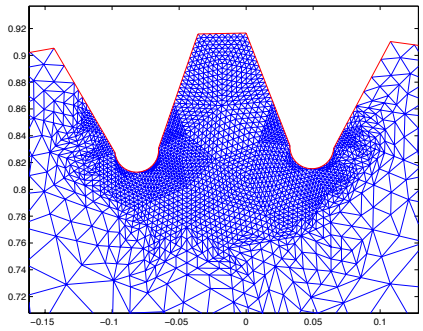

Figure 5: The mesh is refined locally around the loaded tooth.

4. Conclusions and Outlook

We have investigated the use of certain Krylov-modes in a modal based model reduction to capture high-frequency effects from a localized boundary load on a two-dimensional geometrically complex elastic body. We have presented numerical evidence showing that the Krylov-modes significantly enhances the reduction on a coarse mesh, and we have illustrated the effect of mesh refinement.

Current research is aimed at the investigation of other methods to capture localized loads. In the near future we shall begin the evaluation of these methods in 3D. Planned research include error analysis and the construction of adaptive reduction algorithms.

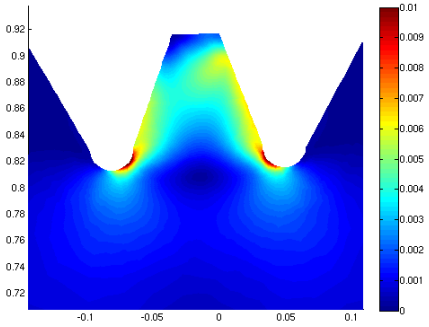

(a) Von Mises stresses of the reference solution $\boldsymbol{u}_h$ on the refined mesh.

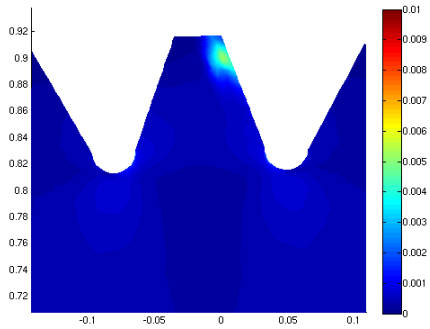

(b) Von Mises stresses on a reduced solution $\boldsymbol{u}_{h,R(20,10)}$ on the refined mesh, using 20 eigenmodes and 10 Krylov-modes.

Figure 6: Von Mises stresses on the reference and reduced solutions on the refined mesh.

References

[1] Zu-Qing Qu. *Model Order Reduction Techniques with Applications in Finite Element Analysis*. Graduate Texts in Mathematics. Springer, London, Berlin, Heidelberg, 2004.

[2] S. Dietz. *Vibration and Fatigue Analysis of Vehicle Systems Using Component Modes*, volume 401. VDI Verlag, 1999.

[3] Yousef Saad. *Iterative Methods for Sparse Linear Systems, 2nd edition*. SIAM, 2003.

[4] The MathWorks, Inc. MATLAB. http://www.mathworks.com/products/matlab/.

[5] Alexandre Ern and Jean-Luc Guermond. *Theory and Practice of Finite Elements*. Graduate Texts in Mathematics. Springer, New York, Berlin, Heidelberg, 2004.

[6] ARPACK. http://www.caam.rice.edu/software/ARPACK/.